European Review for Medical and Pharmacological Sciences 2019; 23: 6011-6017

MiR-140-3p overexpression activates the Wnt signaling pathway to promote fracture healing

Q.-P. LIU, T.-H. WU, H. ZHENG, S.-J. CHEN, Y.-H. CHEN, L. CHEN, Z. LIN

Department of Orthopedics, Mindong Hospital Affiliated to Fujian Medical University, Fu'an, China

Abstract. – OBJECTIVE: To study the mechanism of micro ribonucleic acid (miR)-140-3p participating in the regulation of fracture healing in rats.

MATERIALS AND METHODS: A total of 50 male Sprague-Dawley (SD) rats were randomly divided into five groups, namely, group A [phosphate-buffered saline (PBS)] (n=10), group B (miR-140-3p mimics) (n=10), group C [mimics negative control (NC)] (n=10), group D [antisense oligonucleotide (ASO)-miR-140-3p] (n=10), and group E (ASO NC) (n=10). A rat model of fracture was established on all the rats through the operation. From the successful establishment of the model, the rats in group A were intraperitoneally injected with 50 μL PBS (2 nmol) once a week for 6 weeks, and those in group B, C, D, and E were injected with equivalent volume of miR-140-3p mimics, mimics NC, ASO-miR-140-3p, and ASO NC, respectively, once a week since the successful establishment of model for 6 weeks. The fracture healing in the rats was evaluated via imaging. Meanwhile, Real Time-Polymerase Chain Reaction (RT-PCR) was applied to detect the expression of miR-140-3p in the five groups. Wnt and β-catenin expressions in the five groups were detected by means of Western blotting (WB). Alkaline phosphatase (ALP) and its quantized statistical value in the five groups were detected through immunohistochemical staining.

RESULTS: The expression of miR-140-3p was stimulated in miR-140-3p mimics group and inhibited in ASO-miR-140-3p group. The detection of the miR-140-3p expression level in the five groups via RT-PCR showed that miR-140-3p mimics group had a remarkably higher miR-140-3p expression than the other four groups. The differences were statistically significant ($p<0.05$). The WB assay verified that the Wnt and β-catenin expressions in miR-140-3p mimics group were notably higher than those in control groups, and there were statistically significant differences ($p<0.05$). Compared with those in the groups injected with PBS, ASO miR-140-3p, mimics NC, and ASO NC, there were evidently more callus tissues, better healed and more blurred fracture lines, as well as no translocation and looseness of internal fixation, in the group injected with miR-140-3p mimics, suggesting that the stimulation of the miR-140-3p expression promotes the fracture healing in the rats. The results of immunohistochemical staining indicated that the number of ALP-positive osteoblasts in the rats in miR-140-3p mimics group was increased markedly in comparison with that in the remaining groups ($p<0.05$), implying that the differentiation of osteoblasts in the rats was affected in miR-140-3p mimics group.

CONCLUSIONS: The overexpressed miR-140-3p in the rats with fracture can promote fracture healing by activating the Wnt signaling pathway.

Key Words:
MiR-140-3p, Wnt signaling pathway, Fracture healing.

Introduction

Fracture is an injury that is most likely to occur in humans among the traumatic injuries[1]. In spite of the self-repair capacity of the bone, nonunion or delayed union still occurs in about 10-20% fractures[2]. Therefore, it is urgent to formulate treatment strategies in the process of fracture healing to accelerate skeletal regeneration. Fracture healing is a complex process that mainly consists of four steps: inflammatory response, organization of hematoma, formation of primary callus, and transformation remodeling of callus[3]. The regeneration of fracture healing is precisely composed of hormones, cytokines, chemokines, growth factors, and regulatory factors in each stage.

Micro ribonucleic acids (miRNAs) are a category of small non-coding RNA molecules with a length of 19-25 nucleotides[4]. Lee et al[5] found in *Caenorhabditis elegans* for the first time that the expression of signaling pathway molecules is controlled by multiple factors, including epigenetic factors and miRNA factors. Although miRNAs are small in volume, non-coding RNAs repress gene expression and participate in bone formation after transcription, but there is still little knowledge about the relationship between miRNAs and the Wnt signaling pathway in fracture healing.

Corresponding Author: Zhen Lin, BM; e-mail: lin87zhen@163.com

They can regulate the gene expression level, and a growing amount of evidence has manifested that miRNAs play important roles in skeletal development and homeostasis[6-8]. As a result, these miRNA markers are able to reflect their correlations with skeletal disease, osteoporosis, osteoarthritis, and osteosarcoma. For example, patients with postmenopausal osteoporosis have remarkably decreased miR-503 and notably up-regulated miR-133a in peripheral blood mononuclear cells[9].

There is new evidence that the utilization of specific matrix by osteoblasts is controlled by crucial development and hormone signals[10-13], of which the most important is the Wnt signaling pathway. It exerts vital effects on accumulation of normal bone mass and controls almost all the aspects of the maturation and function of the osteoblasts. The Wnt signaling pathway plays a central role in the coordination of many cell and tissue processes, including proliferation, tissue development and repair, and metabolism[14]. A thorough research approach, known as the Wnt/β-catenin signaling pathway or "normalized" pathway, regulates proteasomal degradation in the transcription factors[15]. Hence, in this study, the potential mechanisms of miR-140-3p and the Wnt signaling pathway in fracture healing in living rats were investigated by establishing a rat model of fracture.

Materials and Methods

Grouping of Laboratory Rats

A total of 50 male Sprague-Dawley rats (aged 12 weeks old and weighting 250-300 g) were selected, which were purchased from Shanghai Silaike Experimental Animal Co., Ltd. (Shanghai, China). All the rats were randomly divided into five groups, group A [phosphate-buffered saline (PBS)] (n=10), group B (miR-140-3p mimics) (n=10), group C [mimics negative control (NC)] (n=10), group D [antisense oligonucleotide (ASO)-miR-140-3p] (n=10), and group E (ASO NC) (n=10). This study was approved by the Animal Ethical Committee of Fujian Medical University.

Establishment of a Rat Model of Fracture and Treatment of Animals in Each Group

After grouping, a model of tibial fracture was established through operation among all the rats. The rats were anesthetized by 3% pentobarbital sodium (30 mg/kg) (Sigma-Aldrich, St. Louis, MO, USA) before the operation. After that, the four limbs of the rats were fixed, the left lower limb was routinely disinfected, the skin and soft tissue were cut open to expose the left tibia, and a transverse fracture at the upper or middle segment of the left tibia was artificially caused using a wire saw. Next, reduction of the fracture site and intramedullary fixation with a 1.0 mm Kirschner wire were conducted. Finally, the wound was rinsed. After the operation, the laboratory rats were intramuscularly injected with 80×104 U penicillin (Shanghai Xianfeng Pharmaceutical Co., Ltd., China, batch number: S100824, Shanghai, China) twice a day for three consecutive days. All the rats were separately raised in a cage without limitation of activities. The laboratory environment was maintained at 21°C, and the light/dark cycle (12/12 h) was controlled. The rats in group A were intraperitoneally injected with 50 μL PBS (2 nmol), and those in group B, C, D, and E were injected with an equivalent volume of miR-140-3p mimics, mimics NC, ASO-miR-140-3p and ASO NC, respectively, once a week since the successful establishment of model for 6 weeks.

Imaging Analysis

After the successful establishment of the rat model of fracture and injection among the five groups of rats, X-ray films of all the rats were obtained to observe the fracture healing on the 49th day, including analyses of the location of internal fixation, formation of callus, and healing of fracture line. The shooting parameters of the X-ray apparatus are set as follows: 50 kV, 50 mA, and 125 mS. Each X-ray film was analyzed by 1 radiologist, 1 laboratory researcher, and 1 orthopedist. The rats were killed by decapitation after the last analysis of their X-ray films. Then, the callus tissue was taken out from the dead rats, placed into a low-temperature tissue storage tube, and quickly added with liquid nitrogen. Meanwhile, it was preserved in an ultra-low-temperature artificial climate box.

Analysis via Real Time-Polymerase Chain Reaction (RT-PCR)

RT-PCR was performed to examine whether there was differential expression of miR-140-3p between group B and control groups A, C, D, and E. The total RNA was extracted using TRIzol reagent (Sangon Biotech, Shanghai, China). NanoDrop 2000 device (Thermo Fisher Scientific, Waltham, MA, USA) was utilized for reverse transcription, and TaKaRa RNA PCR kit (TaKaRa, Dalian, China) and Oligo dT primers (Invitrogen, Carlsbad, CA, USA) were applied to obtain

cDNA samples. The SYBR mixture was utilized to detect the expression level of miR-21 (TaKaRa, Dalian, China) on Light Cycler 480 device (Roche, Basel, Switzerland). Every sample was measured for three times. The design and synthesis of primers are shown in Table I. The expression level of miR-21 was normalized by virtue of glyceraldehyde-3-phosphate dehydrogenase (GAPDH), and the $2^{-\Delta\Delta Ct}$ method was adopted for data analysis.

Western Blotting (WB) Analysis

The callus tissues at the fracture site in control groups and experimental group were rinsed twice with ice-cold normal saline. Then, according to the instructions of total protein extraction kits, the tissues were added with lysis buffer and homogenized in a tissue homogenizer for 1 min, followed by centrifugation at 4°C and 12,000 rpm for 10 min and collection of the supernatant, which was the total protein in the tissues. Next, a bicinchoninic acid (BCA) protein assay kit (Pierce, Rockford, IL, USA) was utilized to determine the protein concentration, followed by subpackaging and preservation at -70°C for standby use. The total protein extracting solution was evenly mixed with 2× loading buffer at a volume ratio of 1:1, followed by boiling water bath for 5 min, natural cooling, and storage in a refrigerator at 4°C for standby use. The separation gel for sodium dodecyl sulfate-polyacrylamide gel electrophoresis (SDS-PAGE) at a proper proportion was prepared in accordance with the molecular weight of target proteins, which was solidified for about 1 h. Then, 5% SDS-PAGE spacer gel was prepared and solidified for about half an hour. After that, electrophoresis buffer was added, and denatured protein samples were added into loading wells according to the protein concentration, so as to ensure the equal content of total proteins in each well. The electrophoresis was performed under a constant voltage of 220 V, which was stopped until the bromophenol blue reached the bottom of the gel. Next, the gel was cut on the basis of the molecular weight of target proteins and then placed into transfer buffer. A layer of polyvinylidene difluoride (PVDF) membrane (Millipore, (Billerica, MA, USA) and 6 layers of filter paper were tailored according to the size of the gel. The PVDF membrane was soaked in methanol for 10 s, and then the PVDF membrane and filter paper were put into the transfer buffer. The anode, three layers of filter paper, PVDF membrane, gel, three layers of filter paper and cathode were placed into a transmembrane apparatus in sequence, and attention was paid that the edges were aligned to prevent blebbing. Then, the membrane transfer was conducted under a constant voltage of 220 V for 2 h. After that, the PVDF membrane with proteins was sealed in a shaking table containing 5% skim milk powder at room temperature for 2 h. The sealed membrane was washed with Tris-Buffered Saline-Tween 20 (TBST) for 5 min, added with a corresponding proportion of primary antibodies, and incubated at 4°C overnight. Next, the membrane was washed with TBST for 3 times (10 min per time), placed into relevant secondary antibodies, incubated on the shaking table at room temperature for 3 h, and washed again with TBST for 3 times (10 min per time). A gel imager was turned on and preheated for 30 min, and A and B reagents in enhanced chemiluminescence (ECL) kit were mixed in equal volume, which were added onto the PVDF membrane in drops to contact completely, followed by color development in the dark for 1 min. Then, excess liquid around the membrane was absorbed by the filter paper, and the membrane was put into the gel imager for photographing under a dynamic integration mode and observation. The image analysis software was utilized for image analysis.

Immunohistochemical Staining

The rats' tibia specimens were fixed and decalcified in a decalcifying solution containing 10% ethylenediaminetetraacetic acid at room temperature for 1 week. After that, the specimens were

Table I. RT-PCR primer sequences for miR-140-3p.

Gene name	Primer sequence
MiR-140-3p-F	ACA CTC CAG CTG GGA GGC GGG GCG CCG
MiR-140-3p-R	CGG GA
U6-F	CTC AAC TGG TGT CGT GGA
U6-R	CTC GCT TCG GCA GCA CA
	AAC GCT TCA CGA ATT TGC GT

rinsed with running water for 2 h and dehydrated in graded alcohol, followed by the embedding of tissues in paraffin. When the paraffin blocks were cooled down, they were sliced to 4 μm-thick sections by virtue of a microtome. The paraffin sections were routinely deparaffinized, rehydrated, sealed in endogenous peroxidase, incubated in 3% H_2O_2 at room temperature for 30 min and rinsed with phosphate-buffered saline (PBS) for 2 min twice, followed by incubation with compound enzyme digestive juice at 37°C for 30 min, washing with PBS for 2 min * 3 times for antigen retrieval, and sealing in serum for 1 h without washing. Then the air-dried liquid was shaken off, and each specimen was added in drops with 50 μL specific primary antibody working solution and incubated in the refrigerator at 4°C for over 17 h, followed by washing with PBS for 5 min * 3 times, addition of secondary antibodies, incubation at 37°C for 1 h, washing again with PBS for 5 min * 3 times, dropwise addition of SABC reagent and incubation at 37°C for 30 min. Subsequently, a drop of diaminobenzidine (DAB) developer was added, the color developing effects were observed under a microscope, and the color development was terminated with distilled water timely, followed by counterstaining with methyl green for 5 min, routine dehydration, clearing, and mounting. Alkaline phosphatase (ALP) was observed and its quantized value was recorded.

Statistical Analysis

All the data in this experiment were expressed by mean ± standard error of mean, and Statistical Product and Service Solutions (SPSS) 21.0 software (IBM, Armonk, NY, USA) was used for the statistical analysis of the experimental results. The *t*-test was adopted for comparison of mean between two groups, and one-way analysis of variance was performed for comparison of the sample mean between groups. $p<0.05$ suggested that the difference was statistically significant.

Results

Imaging Analysis

The imaging evaluation on the 7th week showed that compared with those in the groups injected with PBS, ASO miR-140-3p, mimics NC, and ASO NC, there were evidently more callus tissues, better healed and more blurred fracture lines as well as no translocation and looseness of internal fixation in the group injected with miR-140-3p mimics, suggesting that the overexpression of miR-140-3p promotes the fracture healing in the rats.

MiR-140-3p Expression in Five Groups Detected Via RT-PCR

After the rat model of fracture was established successfully, the rats in group A were intraperitoneally injected with 50 μL PBS (2 nmol), and those in group B, C, D, and E were injected with an equivalent volume of miR-140-3p mimics, mimics NC, ASO-miR-140-3p, and ASO NC, respectively, once a week for 6 weeks. Then, the rats were killed by decapitation, and the expression of miR-140-3p in the five groups of callus tissues was detected *via* RT-PCR.

According to Figure 2, there was no statistically significant difference in the miR-140-3p expression among groups A, C, D, and E ($p>0.05$). The miR-140-3p expression was increased markedly in group B compared with that in groups A, C, D, and E, displaying a statistically significant difference ($p<0.01$).

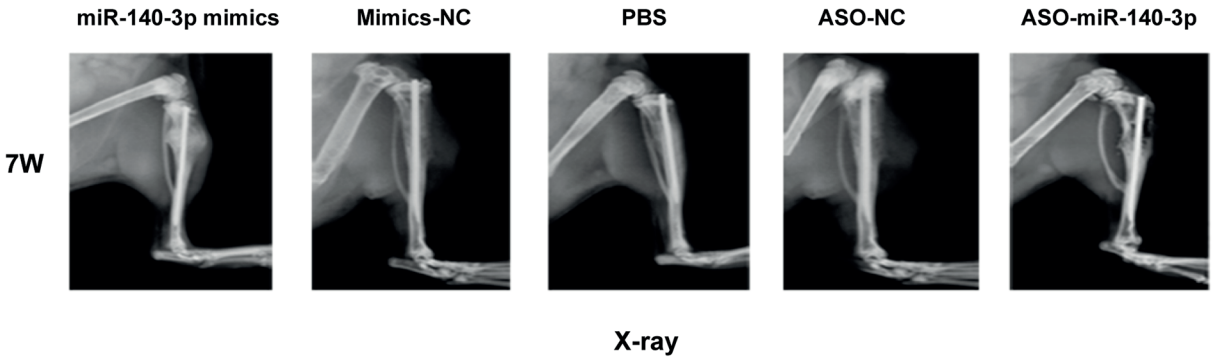

Figure 1. Imaging evaluation.

WB Results

WB assay was adopted to measure the content of Wnt and β-catenin proteins in the callus tissues among the five groups of rats. The expression of Wnt protein in the five groups of callus tissues is shown in Figure 4. MiR-140-3p mimics group had evidently higher Wnt expression than PBS group, ASO miR-140-3p group, mimics NC group, and ASO NC group ($p<0.05$). The expression of the β-catenin protein in the five groups of callus tissues is shown in Figure 3. MiR-140-3p mimics group had notably higher β-catenin expression than PBS group, ASO miR-140-3p group, mimics NC group, and ASO NC group ($p<0.05$).

Immunohistochemical Staining Results

Many factors are involved in the regulation of the differentiation of osteoblasts. For instance, ALP is a marker of early differentiation and maturation of osteoblasts. The immunohistochemical staining results for ALP indicated that the number of ALP-positive osteoblasts in miR-140-3p mimics group was increased markedly in comparison with that in the remaining groups ($p<0.05$), implying that the differentiation of rat osteoblasts is affected in miR-140-3p mimics group.

Discussion

In recent years, the researches on the molecular mechanism of fracture healing become more and more intensive. MiRNAs play crucial roles in the complicated process of regulating osteogenic differentiation and osteoblast formation. To apply miRNAs to clinical treatment, miR-140-3p, a specific miRNA and an iconic regulator of osteogenesis, was included into this study.

Currently, a variety of drugs are researched to promote fracture healing, so as to improve the therapeutic effects of surgical procedures. Among them, the drugs related to the Wnt/β-catenin signaling pathway have been widely paid attention to[16,17]. However, multiple studies over the past few years have pointed out that only the precisely controlled Wnt/β-catenin signaling pathway during fracture healing can guarantee better fracture healing[18-20]. Chen et al[18] discovered that once the mesenchymal stem cells are differentiated into osteoblasts in the fracture repair stage, up-regulating the activity of the Wnt/β-catenin signaling pathway can prominently accelerate the differentiation of osteoblasts and strengthen the bone formation capacity, thereby promoting fracture healing. In the inflammatory phase, however, the Wnt/β-catenin signaling pathway can promote fracture healing only when it is maintained at a proper level, and an excessively high or low level will impair the differentiation of mesenchymal stem cells into osteoblasts[17,21].

In this work, it was found that the expression of miR-140-3p was stimulated in miR-140-3p mimics group and inhibited in the Aso-miR-140-3p group. The detection of miR-140-3p expression level in the five groups *via* RT-PCR showed that miR-140-3p mimics group had a remarkably higher miR-140-3p expression than the other four groups. The WB assay verified that miR-140-3p mimics group had notably increased Wnt and β-catenin expressions than control groups, so it is presumed that miR-140-3p possibly stimulates the Wnt signaling pathway to promote fracture healing. In this experiment, a rat model of fracture was established, the rats in group A were intraperitoneally injected with 50 μL PBS (2 nmol), and those in groups B, C, D, and E were injected with an equivalent volume of miR-140-3p mimics, mimics NC, ASO-miR-140-3p, and ASO NC, respectively. The imaging evaluation manifested

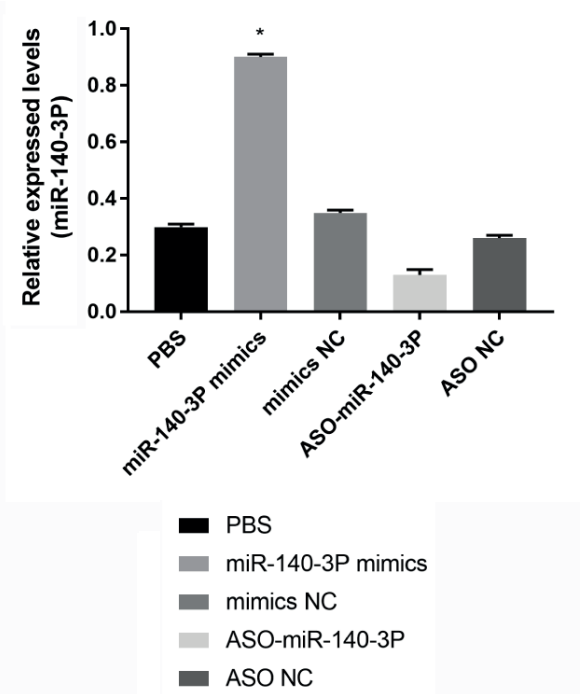

Figure 2. MiR-140-3p expression in five groups detected *via* RT-PCR. MiR-140-3p mimics group, PBS group, ASO miR-140-3p group, mimics NC group and ASO NC group. *$p<0.01$.

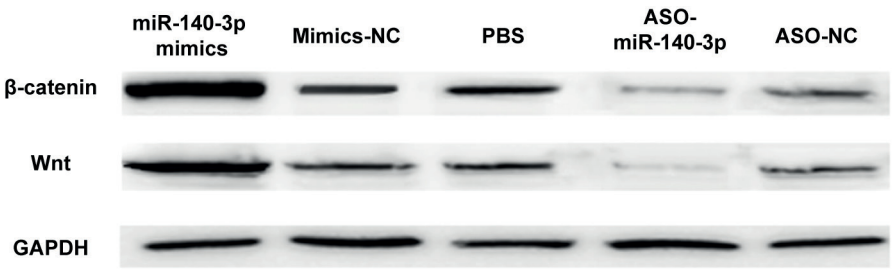

Figure 3. MiR-140-3p mimics group has notably higher β-catenin expression than PBS group, ASO miR-140-3p group, mimics NC group and ASO NC group ($p<0.05$).

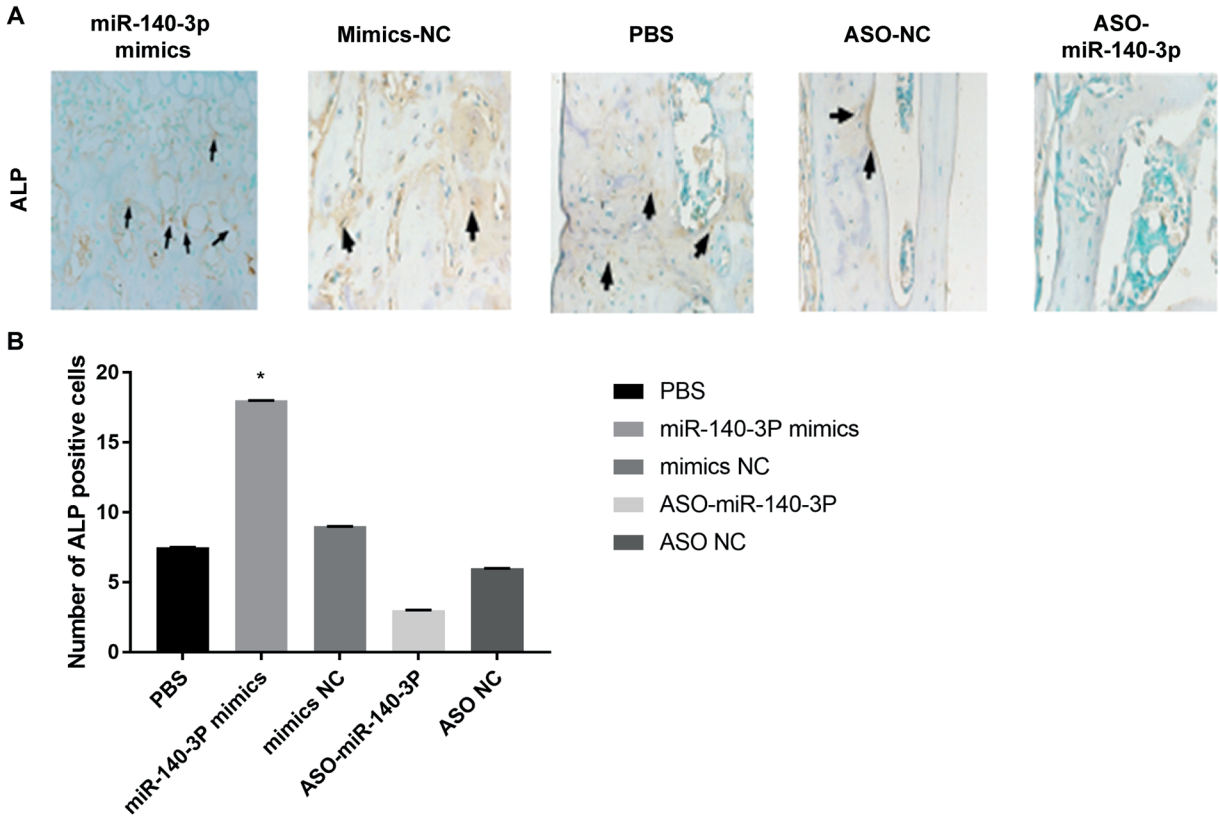

Figure 4. Immunohistochemical staining and statistical results for ALP at the callus in each group of rats at 7 weeks after fracture (***A***), (***B***) (400×). *: $p<0.01$.

that there were evidently more callus tissues, better healed and more blurred fracture lines as well as no translocation and looseness of internal fixation in the group injected with miR-140-3p mimics in comparison with those in groups injected with PBS, ASO miR-140-3p, mimics NC, and ASO NC, implying that the stimulation of miR-140-3p expression promotes the fracture healing in the rats. Meanwhile, the results of immunohistochemical staining indicated that the number of ALP-positive osteoblasts in the rats in miR-140-3p mimics group was increased markedly compared with that in the remaining groups ($p<0.05$), implying that the differentiation of osteoblasts in the rats is affected in miR-140-3p mimics group. Furthermore, it was conjectured by determining

the Wnt and β-catenin proteins that the fracture healing in rats may be promoted by the Wnt signaling pathway.

Conclusions

We assumed that the overexpressed miR-214-3p promotes fracture healing in the rats with fracture by activating the Wnt signaling pathway. An *in-vivo* model was provided in this experiment to further investigate the mechanism of fracture healing, thus laying a foundation for deeper studies on fracture healing in human beings. More subsequent experiments are still needed to explore the mechanism of fracture healing.

Conflict of Interests

The Authors declare that they have no conflict of interests.

References

1) Einhorn TA, Gerstenfeld LC. Fracture healing: mechanisms and interventions. Nat Rev Rheumatol 2015; 11: 45-54.
2) Axelrad TW, Kakar S, Einhorn TA. New technologies for the enhancement of skeletal repair. Injury 2007; 38 Suppl 1: S49-S62.
3) Marsell R, Einhorn TA. The biology of fracture healing. Injury 2011; 42: 551-555.
4) Bartel DP. MicroRNAs: genomics, biogenesis, mechanism, and function. Cell 2004; 116: 281-297.
5) Lee RC, Feinbaum RL, Ambros V. The C. elegans heterochronic gene lin-4 encodes small RNAs with antisense complementarity to lin-14. Cell 1993; 75: 843-854.
6) Kobayashi T, Lu J, Cobb BS, Rodda SJ, McMahon AP, Schipani E, Merkenschlager M, Kronenberg HM. Dicer-dependent pathways regulate chondrocyte proliferation and differentiation. Proc Natl Acad Sci U S A 2008; 105: 1949-1954.
7) Ge DW, Wang WW, Chen HT, Yang L, Cao XJ. Functions of microRNAs in osteoporosis. Eur Rev Med Pharmacol Sci 2017; 21: 4784-4789.
8) Gordon JA, Montecino MA, Aqeilan RI, Stein JL, Stein GS, Lian JB. Epigenetic pathways regulating bone homeostasis: potential targeting for intervention of skeletal disorders. Curr Osteoporos Rep 2014; 12: 496-506.
9) Wang Y, Li L, Moore BT, Peng XH, Fang X, Lappe JM, Recker RR, Xiao P. MiR-133a in human circulating monocytes: a potential biomarker associated with postmenopausal osteoporosis. PLoS One 2012; 7: e34641.
10) Fulzele K, Riddle RC, DiGirolamo DJ, Cao X, Wan C, Chen D, Faugere MC, Aja S, Hussain MA, Bruning JC, Clemens TL. Insulin receptor signaling in osteoblasts regulates postnatal bone acquisition and body composition. Cell 2010; 142: 309-319.
11) Li Z, Frey JL, Wong GW, Faugere MC, Wolfgang MJ, Kim JK, Riddle RC, Clemens TL. Glucose transporter-4 facilitates insulin-stimulated glucose uptake in osteoblasts. Endocrinology 2016; 157: 4094-4103.
12) Dirckx N, Tower RJ, Mercken EM, Vangoitsenhoven R, Moreau-Triby C, Breugelmans T, Nefyodova E, Cardoen R, Mathieu C, Van der Schueren B, Confavreux CB, Clemens TL, Maes C. Vhl deletion in osteoblasts boosts cellular glycolysis and improves global glucose metabolism. J Clin Invest 2018; 128: 1087-1105.
13) Stegen S, van Gastel N, Eelen G, Ghesquiere B, D'Anna F, Thienpont B, Goveia J, Torrekens S, Van Looveren R, Luyten FP, Maxwell PH, Wielockx B, Lambrechts D, Fendt SM, Carmeliet P, Carmeliet G. HIF-1alpha promotes glutamine-mediated redox homeostasis and glycogen-dependent bioenergetics to support postimplantation bone cell survival. Cell Metab 2016; 23: 265-279.
14) Clevers H. Wnt/beta-catenin signaling in development and disease. Cell 2006; 127: 469-480.
15) Angers S, Moon RT. Proximal events in Wnt signal transduction. Nat Rev Mol Cell Biol 2009; 10: 468-477.
16) Chen Y, Alman BA. Wnt pathway, an essential role in bone regeneration. J Cell Biochem 2009; 106: 353-362.
17) Agholme F, Aspenberg P. Wnt signaling and orthopedics, an overview. Acta Orthop 2011; 82: 125-130.
18) Chen Y, Whetstone HC, Lin AC, Nadesan P, Wei Q, Poon R, Alman BA. Beta-catenin signaling plays a disparate role in different phases of fracture repair: implications for therapy to improve bone healing. PLoS Med 2007; 4: e249.
19) Liedert A, Rontgen V, Schinke T, Benisch P, Ebert R, Jakob F, Klein-Hitpass L, Lennerz JK, Amling M, Ignatius A. Osteoblast-specific Krm2 overexpression and Lrp5 deficiency have different effects on fracture healing in mice. PLoS One 2014; 9: e103250.
20) Agholme F, Isaksson H, Kuhstoss S, Aspenberg P. The effects of Dickkopf-1 antibody on metaphyseal bone and implant fixation under different loading conditions. Bone 2011; 48: 988-996.
21) Baron R, Rawadi G. Targeting the Wnt/beta-catenin pathway to regulate bone formation in the adult skeleton. Endocrinology 2007; 148: 2635-2643.